JOURNAL OF MASS SPECTROMETRY, VOL. 32, 714–722 (1997)

Profile and Flight Time Analysis of Bovine Insulin Clusters as a Probe of Matrix-assisted Laser Desorption/Ionization Ion Formation Dynamics

Gary R. Kinsel,[1] Ricky D. Edmondson[2] and David H. Russell[2]*

[1] Department of Chemistry and Biochemistry, The University of Texas at Arlington, Arlington, Texas 76019-0065, USA
[2] Department of Chemistry, Texas A & M University, College Station, Texas 77843-3325, USA

Detailed ion signal profile and flight time analyses were performed on the time-of-flight signals obtained for bovine insulin cluster ions produced by matrix-assisted laser desorption/ionization (MALDI). Profile analyses of the ion signals strongly suggest that the signals are made up of a composite of two separate components and analysis of the flight times of the two components suggests that the ions are formed with different dynamics. The formation dynamics of one component of the ions is best described as prompt ionization to yield ions with essentially mass-independent total energies. The formation dynamics of the second component of the ions is best described as delayed gas-phase ionization of entrained material moving at a constant velocity. This model is supported by several ancillary experiments and suggests new insights into the mechanism of MALDI ion formation. © **by John Wiley & Sons, Ltd.**

J. Mass Spectrom. **32**, 714–722 (1997)
No. of Figures: 5 No. of Tables: 2 No. of Refs: 11

KEYWORDS: ion formation dynamics; matrix-assisted laser desorption/ionization; bovine insulin clusters; ion signal profile analysis; flight time analysis

INTRODUCTION

Understanding the dynamics of ion formation in matrix-assisted laser desorption/ionization (MALDI) remains an important goal. The dynamics of ion formation are intimately linked to the temporal width of the ion signal in time-of-flight (TOF) mass spectrometry and, to a large extent, dictate the relative success of various instrumental approaches to improving MALDI/TOF mass accuracies and/or signal resolutions. Furthermore, the dynamics of ion formation can provide important insights into the mechanism(s) of ion formation. Specifically, the distributions in initial ion translational energy, position of ion formation in the mass spectrometer source region and/or temporal duration over which the ions are formed provide a framework into which any model of the MALDI ion formation process must fit.

In principle, profile analysis of ion signals recorded in a linear TOF mass spectrometer can be used to probe the dynamics of ion formation. The flight time (*f.t.*) of an ion of a particular mass in a given TOF mass spectrum is directly related to both the total translational energy of the ion and the time required for ion formation. The total translational energy of the ion, in turn, is related to the initial kinetic energy of the ion and the position in the source region electric field at which the ion is produced. However, deconvolution of a single TOF ion signal profile to extract the specific dynamic information is inherently difficult owing to the interdependent effects of variations in ion formation parameters on the *f.t.* of a given ion. For example, the arrival of an ion of a given mass at a longer *f.t.* relative to another ion of equal mass can be equally interpreted as delayed formation of the late-arriving ion or as the late-arriving ion having less total translational energy. Furthermore, without the availability of calibrating ion signals having known ionization dynamics and/or very accurate parameterization of the TOF instrumentation, assignment of an absolute energy scale to the *f.t.* distribution of the ion signals is highly speculative.

One approach to circumventing some of these difficulties is to examine trends in the *f.t.* behavior for ion signals covering an extended mass range. If ions of two different masses are assumed to be formed via similar dynamics, then the *f.t.* of each of these two ion signals can be used to predict the *f.t.* of a third ion signal. Deviations in the *f.t.* of the third ion signal from the predicted value can be interpreted as resulting from changes in the total translational energy of the ions and/or changes in the time required for ion formation. This approach has been used by Nelson *et al.*[1] in a study of the systematic changes in *f.t.* of high molecular mass multiply charge human immunglobulin ions produced by MALDI. In this study, systematic decreases in the *f.t.* of the higher mass cluster ions from predicted values was

* Correspondence to: D. H. Russell, Department of Chemistry, Texas A & M University, College Station, Texas 77843-3325, USA.
Contact grant sponsor: US Department of Energy, Division of Chemical Sciences, Office of Basic Energy Science.
Contact grant sponsor: National Science Foundation.

CCC 1076–5174/97/070714–09 $17.50

Received 1 November 1996
Accepted 10 March 1997

interpreted as resulting from systematic increases in total ion energy.

Flight time analysis relies on the relationship between ion *f.t.* and mass. That is, the analysis makes use of the fundamental relationship $E = \frac{1}{2}mv^2$ which can be rearranged to give

$$f.t. = [l/(2E)^{1/2}]m^{1/2} \quad (1)$$

where m is the mass of the ion, l is the ion flight path and E is the total ion translational energy. In a typical TOF spectrum the experimentally recorded *f.t.* is shifted by an offset resulting from the timing delay between the actual ion formation event and the start of spectrum acquisition. Thus, an additional offset constant, b, is generally added to Eqn (1) to account for this delay. It is important to note, however, that this offset constant can also incorporate temporal delays in the formation of the ions. For example if all ions are formed a fixed amount of time after the initial excitation event, this delay in ion formation would be absorbed in the offset constant. Finally, if all ions travel the same distance, l, and all ions achieve the same most probable translational energy, E, then the conventional TOF calibration equation is obtained:

$$f.t. = km^{1/2} + b \quad (2)$$

From the derivation of this equation, it can be seen that deviations in the *f.t.* of high-mass ions from predicted values can arise from variations in any of the three parameters, l, E or b. Given the still obscure understanding of the dynamics of MALDI ion formation, it is important to consider the possible contribution of all of these effects to deviations in predicted ion flight times.

In this paper, we describe experiments in which we probed the dynamics of MALDI ion formation through examinations of both the profiles and flight times of MALDI ion signals. These studies were performed on MALDI/TOF spectra of clusters of bovine insulin where the mass range of the cluster ions extends over nearly one order of magnitude. Initially, the conventional TOF calibration equation was applied to the range of cluster ion flight times to assess the linearity of the response and the magnitude of the temporal offset constant. In further analyses, a variety of methods for defining the TOF of the cluster ion signals were developed through deconvolution of the profiles of the cluster ion signals. Subsequent application of the calibration equation to the deconvoluted signal profiles suggested a systematic, mass-dependent change in the ion signal flight times for one component of the ion signals, but not for a second component. Ultimately, this analysis allows the development of a model of ion formation which combines several aspects of previously suggested models of MALDI ion formation with unique insights gains from these studies. Specifically, the data suggest that ions produced by MALDI consist of two distinct components, one the result of surface or near-surface ionization with no systematic mass-dependent initial kinetic energy and the other the result of gas-phase ionization of material moving at a nearly mass-independent constant velocity. This model is further supported by several ancillary experiments which yields results consistent with predicted behavior.

EXPERIMENTAL

MALDI was performed in a 1 m linear TOF mass spectrometer designed and constructed in-house. Details of the instrument have been presented previously and only a few specific experimental parameters pertinent to the results presented will be described.[2] Briefly, the source region of the TOF mass spectrometer consisted of a repeller and two extraction electrodes, each separated by 1 cm. Each of the 5 cm diameter extraction electrodes had a 1 cm hole bored through the middle of the electrode for transmission of the MALDI ions. These holes were covered with 90% transmission Ni mesh to delineate the associated electric fields cleanly. The repeller was typically biased to +20 000 V and the second extraction electrode was maintained at ground. The potential applied to the first extraction electrode could be varied from ground to +20 000 V. In the deceleration/re-acceleration experiments additional extraction electrodes were added to the ion source region or placed in the flight path of the ions. These electrodes were identical with the source region extraction electrodes having 1 cm holes covered by 90% transmission Ni mesh to delineate the associated electric fields cleanly. In the retarding field experiments the voltage from a single power supply was applied to both the repeller and the deceleration electrodes. In this manner, the voltage applied to both electrodes was kept identical. All ions were detected using a dual microchannel plate detector located 1 m from the ion source region. Background pressures in the instrument were maintained at 2×10^{-7}–4×10^{-7} Torr (1 Torr = 133.3 Pa) during acquisition of all TOF spectra.

All samples were prepared using conventional procedures. Specifically, 2 μl of a 15 mg ml^{-1} solution of α-cyano-4-hydroxycinnamic acid in methanol was mixed with 1 μl of a 1 mg ml^{-1} solution of bovine insulin in methanol containing 1% trifluoroacetic acid directly on the surface of a stainless-steel probe and allowed to air dry. MALDI ions were generated by focusing the output of a pulsed nitrogen laser (337 nm) on to the surface of the sample probe which protruded through a hole in the repeller electrode such that the surface of the sample probe was flush with the surface of the repeller electrode. Desorbing laser energies of 50 μJ per pulse were focused to $\sim 200 \times 500$ μm to yield desorbing energy densities of 50 mJ cm^{-2}. It should be noted that cluster ion spectra such as those shown in this paper were strongly dependent on the desorbing laser energy density and careful control of this parameter is needed to acquire satisfactory cluster ion mass spectra.

The ion signal vs TOF spectrum was acquired using a 100 MHz LeCroy 9400 oscilloscope. Data acquisition was triggered by a fast photodiode positioned to detect a reflection of the desorbing laser pulse. Typically, the TOF spectra from 100 individual laser pulses were averaged to produce the spectra discussed in this paper. The averaged TOF spectra were transferred from the oscilloscope to a personal computer where subsequent data analysis was performed. Curve fitting of the cluster ion signal profiles was carried out using the Levenberg–

Marquardt algorithm contained in GRAMS 386 software supplied by Galactic Industries.[3] The segments of the TOF spectra containing the ion signal profiles to be analyzed typically contained 500–600 data points (5–6 μs in length), allowing ~1 μs of baseline on each side of the peak, as shown in Fig. 2. Single- and multi-component curve fitting were achieved by iteratively calculating peak widths and positions leading to a minimization of the residual with respect to the actual data.

RESULTS AND DISCUSSION

Single-component fits to ion signal profiles

As discussed in the Introduction, for MALDI ions covering an extended mass range, systematic variations in the length of the ion flight path, the total translational energy or the temporal offset in ion formation can lead to a non-linear relationship between ion *f.t.* and $m^{1/2}$. To test the linearity of the relationship between *f.t.* and $m^{1/2}$, we applied the TOF calibration equation to the ion signals recorded for singly charged bovine insulin cluster ions produced by MALDI. Figure 1 shows a representative MALDI/linear TOF mass spectrum of the singly charge bovine insulin cluster ions, $(BI)_n^+$, where $n = 1$–14 are easily observed. Using the flight times for the maximum intensity of each of the cluster ions from $(BI)_2^+$ to $(BI)_{10}^+$ and the square root of the exact mass of the most abundant isotope of each of these cluster species, we performed a linear regression to determine the TOF calibration constants. (The data for the unclustered BI^+ were not included in this treatment since the BI^+ ion signals were frequently saturated and their profiles distorted.)

Table 1 gives the data used to obtain the best fit parameters and the calculated calibration constants, k and b. Table 1 also gives the back-calculated masses obtained by inputting the ion signal flight times into the best fit TOF calibration equation and the error in the back-calculated masses. These last two columns are a measure of how well the linear calibration equation fits the entire range of acquired data. Two important insights can be drawn from these data and similar treatments of four additional bovine insulin cluster ion mass spectra. First, no discernible systematic trend exists in the errors in the back-calculated cluster ion masses. A systematic, mass-dependent increase or decrease in the initial cluster ion translational energies would be expected to lead to significant curvature in the *f.t.* vs $m^{1/2}$ plots, resulting in systematic positive and negative errors in the back-calculated masses. Second, while the fit of the TOF calibration equation to the entire range of cluster ion signals is relatively good (average absolute percentage errors in the back-calculated masses for the five spectra analyzed were $0.10 \pm 0.05\%$), the average offset constant, b, of 110 ± 60 ns (obtained from the intercepts of the plots) is inconsistent with our experimental apparatus. Under ideal conditions this value should reflect the experimental delay between firing the desorbing laser and beginning the TOF spectrum acquisition which for our instrumental approach should be no more than 10–20 ns. (We have measured this value

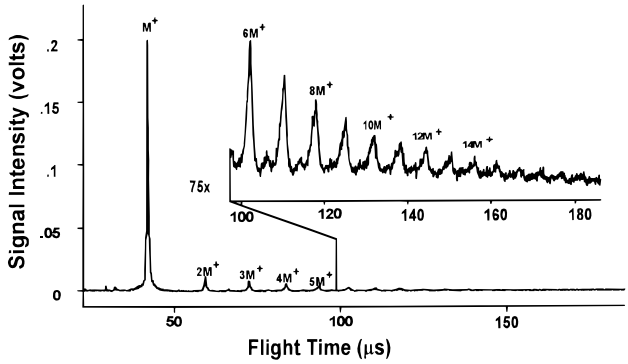

Figure 1. High-mass region of MALDI/TOF spectrum of bovine insulin cluster ions. See text for spectrum acquisition conditions.

Table 1. Calibration of the TOF spectrum of bovine insulin cluster ions[a] using the flight times associated with the maximum intensity of the cluster ion signal

Cluster size $(BI)_n^+$	Cluster mass	Ion flight time (μs)	Calculated mass	Error in calculated mass	% Error
2	11 467.19	59.035	11 465.01	−2.18	−0.019
3	17 200.79	72.235	17 180.14	−20.65	−0.120
4	22 934.38	83.475	22 954.65	20.27	0.088
5	28 667.97	93.275	28 670.89	2.92	0.010
6	34 401.56	102.155	34 398.79	−2.77	−0.008
7	40 135.15	110.395	40 180.98	44.98	0.112
8	45 868.75	117.915	45 848.05	−20.70	−0.045
9	51 602.34	125.115	51 625.08	22.74	0.044
10	57 335.93	131.795	57 291.34	−44.59	−0.078
$k = 0.55004$, $b = 140$ ns[b]			Average absolute error		0.06[c]

[a] This data set was obtained from the mass spectrum shown in Fig. 1.
[b] The average intercept value from the analysis of five mass spectra is 110 ± 60 ns.
[c] The average absolute percentage error in back-calculated cluster ion mass from the analysis of five mass spectra is 0.10 ± 0.05%.

in separate photoionization experiments and confirmed that the b value should be no greater than this indicated range.) As pointed out earlier, this larger than expected b value could be obtained as a result of a mass-dependent ion kinetic energy leading to curvature of the *f.t.* vs $m^{1/2}$ relationship or as a result of delays in the formation of ions relative to firing of the desorbing laser.

Two-component fits to ion signal profiles

With the above observations in mind, the method by which we assigned the flight times of the bovine insulin cluster ions was evaluated. This decision was predicated on the somewhat arbitrary nature of assigning flight times based on maximum signal intensities i.e. increasing relative noise with decreasing cluster ion signal intensity makes this approach less reliable for the larger cluster ion signals. Initially, attempts were made to fit the cluster ion signals to a single Gaussian profile. This decision was based on the expected isotopic distributions calculated for the bovine insulin cluster ions ($(BI)_n^+$ where $n > 2$), which clearly show that a Gaussian profile adequately represents the expected distribution of ion signals. However, it quickly became apparent that this approach gave poor fits to the cluster ion signal profiles. Figure 2 shows expanded views of (a) the $(BI)_2^+$, (b) the $(BI)_3^+$ and (c) the $(BI)_5^+$ cluster ion signals. A non-Gaussian profile is observed for the $(BI)_3^+$ ion signal and distinct asymmetry is observed in the profiles of $(BI)_2^+$ and $(BI)_5^+$. The asymmetric profiles become even more pronounced for the higher n cluster ions (see Fig. 1).

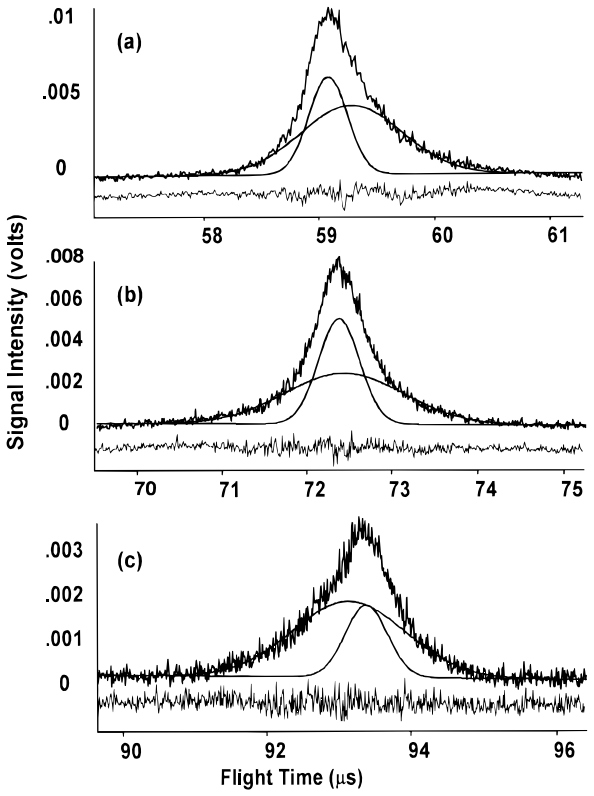

Figure 2. Expanded ion signal profiles from the TOF spectrum shown in Fig. 1. (a) Insulin dimer, $(BI)_2^+$, with two-component Gaussian fit and residual; (b) insulin trimer, $(BI)_3^+$, with two-component Gaussian fit and residual; (c) insulin pentamer, $(BI)_5^+$, with two-component Gaussian fit and residual.

Motivated by the observed cluster ion signal asymmetries, a variety of single- and multi-component curve fits were applied to the bovine insulin cluster ion signals. From these studies it was found that the best fit to the entire range of cluster ion signal profile was obtained using a two-component Gaussian profile (see Fig. 2). Attempts to fit the cluster ion signal profiles using three or greater component Gaussian profiles, single-component or multi-component non-Gaussian profiles generally gave no significant improvement to the fits of the overall data sets (R^2 values improved on average by less than 1%). For example, using a three-component Gaussian profile rather than a two-component Gaussian profile resulted in an average improvement in the R^2 values of 0.15%, with the improvement coming predominantly as a result of fitting of the slight curvature of the baseline rather than the ion signal profile itself. The combination of the two Gaussian distributions gave excellent fits ($R^2 > 0.94$) to all of the bovine insulin cluster ion signals.

Sharp component of ion signal profiles

A distinctive trend was observed in the two Gaussian profiles which gave the best fit to the ion signal profiles. Each two-component fit consisted of one relatively broad profile, which influenced the base width of the ion signal, and one relatively narrow profile, which defined the better resolved upper portion of the ion signals (see Fig. 2). Because of the distinctive nature of the two Gaussian components which made up the curve fits to the ion signal profiles, the TOF calibration equation was applied to the narrow and broad components independently. Tables 2 and 3 give the data used to obtain the best fit parameters and the calculated calibration constants, k and b, for the narrow and broad Gaussian profiles fit to the ion signals in the mass spectrum shown in Fig. 1. Similarly to Table 1, back-calculated masses and errors in back-calculated masses are also given in Tables 2 and 3. It is immediately apparent from this information that application of the TOF calibration equation to the narrow Gaussian components of the bovine insulin cluster ion signals (Table 2) gives significantly lower errors in the calculated cluster ion masses. The average absolute percentage error in the back-calculated mass values is improved by a factor of three for the mass spectrum shown using the flight time of the narrow Gaussian component for determination of the calibration constants. For all five cluster ion mass spectra the average absolute percentage error obtained using the narrow Gaussian component for spectrum calibration was $0.04 \pm 0.03\%$ whereas that using maximum signal intensities was $0.10 \pm 0.05\%$.

Of much greater significance is the value returned for the calibration offset constant, b. For the spectrum in Fig. 1, the b value is reduced from 140 to 36 ns by using the narrow Gaussian component for spectrum mass calibration. For the five cluster ion spectra the average b value for the calibration using the flight times of the narrow Gaussian component is 0.0 ± 30 ns, a value in exact agreement with our experimental approach. Both

Table 2. Calibration of the TOF spectrum of bovine insulin cluster ions[a] using the flight times associated with the sharp component of the two-component Gaussian fits to the cluster ion signals

Cluster size $(BI)_n^+$	Cluster mass	Ion flight time (μs)	Calculated mass	Error in Calculated mass	% Error
2	11 467.19	59.034	11 465.88	−1.30	−0.011
3	17 200.79	72.287	17 195.87	−4.19	−0.029
4	22 934.38	83.472	22 932.31	−2.07	−0.009
5	28 667.97	93.325	28 668.20	0.23	0.001
6	34 401.56	102.246	34 413.48	11.92	0.035
7	40 135.15	110.436	40 149.51	14.36	0.036
8	45 868.75	118.048	45 876.96	8.21	0.018
9	51 602.34	125.185	51 593.77	−8.575	−0.017
10	57 335.93	131.945	57 318.07	−17.86	−0.031
$k = 0.55097$, $b = 36$ ns[b]			Average absolute error		0.02[c]

[a] This data set was obtained from the mass spectrum shown in Fig. 1.
[b] The average intercept value from the analysis of five mass spectra is 0.0 ± 30 ns.
[c] The average absolute percentage error in back-calculated cluster ion mass from the analysis of five mass spectra is 0.04 ± 0.03%.

the linearity of the *f.t.* vs $m^{1/2}$ relationship (implicit in the low average absolute percentage errors) and the near zero value obtained for the offset constant demand that two conditions must be satisifed for the ions which arrive at the most probable flight time of the narrow Gaussian component. First, these ions must be formed within 30 ns of the laser irradiation of the sample surface. Second, little or no systematically increasing or decreasing mass-dependent kinetic energy can be associated with the narrow Gaussian component of the ion signals. These results do not imply that the initial kinetic energy associated with the laser desorbed ions is zero or that the distribution of ion kinetic energies is narrow. These results merely require that, if the ions making up the narrow Gaussian component are desorbed with an initial kinetic energy or distribution of energies, this energy must be nearly the same across the entire cluster ion mass range.

Broad component of ion signal profiles

Interpretation of the formation dynamics associated with the ions making up the broad Gaussian component (Table 3) is more problematic. Several possible explanations for this component are inconsistent with the range of observed behavior for broad Gaussian component flight times. For example, for $(BI)_2^+$ the broad Gaussian component is at longer flight times relative to the narrow Gaussian component. (Note, although not included in this analysis, that the asymmetric broadening of the BI^+ and BI^{2+} is also to longer flight times.) This broadening might be explained as simply the result of unresolved cationized and matrix adducted species. However, there is clearly a progressive shift in arrival of the broad Gaussian component from flight times longer than to flight times shorter than the

Table 3. Calibration of the TOF spectrum of bovine insulin cluster ions[a] using the flight times associated with the broad component of the two-component Gaussian fits to the cluster ion signals

Cluster size $(BI)_n^+$	Cluster mass	Ion flight time (μs)	Calculated mass	Error in Calculated mass	% Error
2	11 467.19	59.129	11 446.31	−20.88	−0.182
3	17 200.79	72.291	17 201.88	1.09	0.006
4	22 934.38	83.354	22 943.64	9.26	0.040
5	28 667.97	93.093	28 680.92	12.95	0.045
6	34 401.56	101.941	34 447.72	46.16	0.134
7	40 135.15	110.058	40 202.56	67.41	0.168
8	45 868.75	117.500	45 869.26	0.51	0.001
9	51 602.34	124.298	51 371.99	−230.35	−0.446
10	57 335.93	131.396	57 450.13	114.20	0.199
$k = 0.54459$, $b = 865$ ns[b]			Average absolute error		0.14[c]

[a] This data set was obtained from the mass spectrum shown in Fig. 1.
[b] The average intercept value from the analysis of five mass spectra is 700 ± 200 ns.
[c] The average absolute percentage error in back-calculated cluster ion mass from the analysis of five mass spectra is 0.14 ± 0.11%

narrow Gaussian component—behavior inconsistent with an adduction model of peak broadening.

The progressive shift in the relative position of the broad Gaussian component is also difficult to reconcile with an explanation of peak broadening as a result of metastable processes. Metastable decay of the cluster ions in the mass spectrometer source region could lead to broadening of the cluster ion signals to either shorter or longer flight times depending on whether the decay occurs early or very late in the cluster ion acceleration. The observed broadening of the low-mass cluster ion signals to longer flight times would require that this broadening result from rapid metastable dissociation of higher mass cluster ions to form these species. On the other hand, the observed broadening of the high-mass cluster ion signals to shorter flight times would require that this broadening results from very slow dissociation of these species to lower mass clusters. It therefore seems unlikely that metastable decay of the cluster ions will lead to the systematic behavior observed experimentally for the broad Gaussian component.

A two-component model of MALDI ion formation

Although the above explanations for the broad Gaussian component cannot be conclusively eliminated, an alternative explanation can be suggested which is consistent with the entire range of behavior of the broad Gaussian component. In terms of energy, the temporal position of the broad relative to the narrow Gaussian component suggests that at low mass the ions making up the broad component have most probable energies that are less than the narrow component. As the mass of the cluster ion increases, however, the most probable energy of the ions making up the broad component progressively increases until it meets and exceeds the most probable energy of the ions making up the narrow component. A viable model to explain this apparent trend in energies of the broad component ion can be synthesized from suggested interpretations of previously reported measurements of kinetic energies of MALDI ions. It should be emphasized that implicit in this model is the assumption that the sharp component ions are made at or near the surface of the probe and are accelerated to the same mass-independent total energy—an assumption strongly supported by the near zero value of the offset constant and linearity of the *f.t.* vs $m^{1/2}$ relationship for these ions.

Essentially two approaches have been employed to measure the kinetic energies of MALDI ions, both yielding apparently contradictory results. In the first approach, several groups have shown that MALDI ions produced in an electric field free region traverse the short region at a constant, mass-independent velocity.[4] Collisional entrainment of the ions in an expanding plume of high-velocity laser desorbed material has been suggested as an explanation of this behavior and various reports have placed the entrainment velocity at between 500 and 1200 m s^{-1}.[5] The implication of MALDI ions being produced with a constant, mass-independent velocity is that the total ion kinetic energy increases with increase in the m/z of the ion. It is important to recognize, however, that these experiments could not indicate the position in the field-free region at which the MALDI ions are formed, i.e. proton and/or cation attachment to form the product ions observed in the mass spectrum can occur at the probe surface or at any point in the electric field-free region and the final experimental result would be indistinguishable. Furthermore, general interpretation of these results with regard to conventional MALDI assumes that the source region electric field strength has no influence on the mechanism or dynamics of ion formation.

In the second approach, kinetic energies of MALDI ions produced under conventional high accelerating electric field conditions have been measured by both retarding field[6] and electrostatic analyzer studies.[7] These studies show that MALDI ions produced in strong accelerating electric fields can exhibit substantial kinetic energy deficits relative to the applied accelerating voltage. The energy deficits were attributed to both delayed gas-phase ion formation and to kinetic energy loss resulting from collisions of promptly formed ions with simultaneously desorbed neutral material. However, these studies were performed under conditions where the MALDI ion kinetic energies were measured at a relatively long distance from the ion source region, e.g. by the potential applied to a reflecting ion mirror $\sim$1 m from the ion source region of by an electrostatic analyzer $\sim$2.4 m from the ion source region. The implicit assumption of these measurements is that no systematic discrimination against high or low ion kinetic energies is introduced under these conditions. This assumption may be called into question, however, if, for example, high kinetic energy ions are collected less efficiently or contain concomitant high internal energies and undergo metastable decay while traversing the region between the ion source and the kinetic energy analyzer.

The energetic behavior of the broad component ions in the bovine insulin cluster ion signal profiles appear to exhibit characteristics associated with both postulated models. That is, for the low-mass cluster ions, the kinetic energy deficit associated with the broad component ions is consistent with a model of delayed gas-phase ion formation or collisional energy loss. Across the entire range of cluster ion masses, however, the broad component ions exhibit a progressive increase in kinetic energy consistent with a model of a constant entrainment velocity. A combination of these two models would be expected to produce results similar to those obtained experimentally for the broad component ions. Specifically, if the ions which make up the broad component of the cluster ion profiles are the result of gas-phase ionization in a plume of entrained material moving at a constant velocity than the observed energetic behavior can be easily interpreted. The total energy, E, of an ion of mass, m, produced by this mechanism will be given by

$$E = E_{ACC} + \tfrac{1}{2}(m)v_{ENT}^2 - d_{GPI}F \qquad (3)$$

where E_{ACC} is the accelerating potential energy, v_{ENT} is the entrainment velocity, d_{GPI} is the distance between the probe surface and the point in the gas phase where ionization occurs and F is the source region electric field. At low mass the added energy resulting from constant-velocity entrainment is exceeded by the energy

deficit resulting from delayed gas-phase ionization at a lower potential energy in the ion source region. As the mass of the ion increases, however, the constant velocity energy term gradually compensates for and exceeds the gas-phase ionization energy loss term.

In order to extract values for v_{ENT} and d_{GPI} from the experimental data, it is necessary to derive a relationship between the flight time errors for the broad component ions and the v_{ENT} and d_{GPI} values. From Eqn (3), it can be seen that

$$\Delta E = E - E_{ACC} = \tfrac{1}{2}(m)v_{ENT}^2 - d_{GPI}F \qquad (4)$$

and that a plot of ΔE vs $\frac{1}{2}(m)$ should give a straight line with a slope equal to v_{ENT}^2 and an intercept equal to $-d_{GPI}F$. If it is assumed that $E_{sharp} \approx E_{ACC}$, then it can be seen from the TOF calibration equation that, to a first approximation, ΔE is related to the flight time errors by

$$\Delta E = E_{broad} - E_{sharp} = \left[\frac{1}{2}(m)\left(\frac{l}{f.t._{broad}}\right)^2 + b\right] - \left[\frac{1}{2}(m)\left(\frac{l}{f.t._{sharp}}\right)^2 + b\right] = \tfrac{1}{2}(m)l^2\left(\frac{1}{f.t._{broad}^2} - \frac{1}{f.t._{sharp}^2}\right) \qquad (5)$$

Thus, Eqn (5) allows the calculation of ΔE for each $(BI)_n^+$ from the flight times of the sharp and broad components and a measurement of the total flight path, l, for the ions. Since the recorded $f.t._{broad}$ also incorporates the temporal delay in ion formation, which is equal to d_{GPI}/v_{ENT}, successive calculations need to be performed until the d_{GPI} and v_{ENT} values converge.

Figure 3 shows the result of the application of this type of analysis to the broad component ion flight times taken from the mass spectrum in Fig. 1. The plot of ΔE vs $\frac{1}{2}(m)$ gives a straight line ($R^2 = 0.96$) with the largest deviations at the highest and lowest cluster ion masses. From the square root of the slope of this line the converged value for v_{ENT} is found to be 980 m s^{-1}. If the source region electric field is taken to be 20 000 V cm^{-1}, d_{GPI} can be calculated from the converged intercept

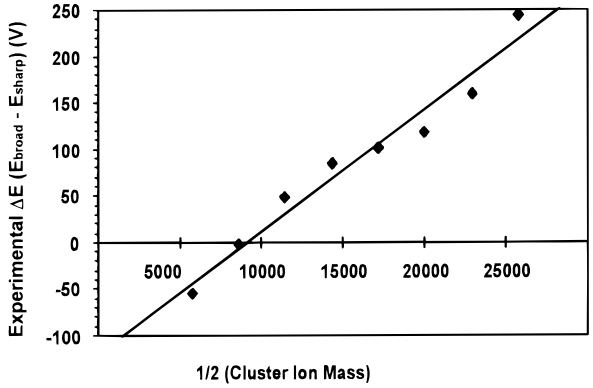

Figure 3. A plot of ΔE vs $\frac{1}{2}(m)$ for the broad component ions in the two-component fits to the bovine insulin cluster ion signal profiles. ΔE is calculated from the difference in the broad and sharp component flight times. From the slope of the line the entrainment velocity, v_{ENT}, can be calculated and from the intercept of the line the point of gas-phase ionization, d_{GPI}, can be calculated (see text for explanation). Reduction of these data taken from the TOF spectrum in Fig. 1 gives $v_{ENT} = 980$ m s^{-1} and $d_{GPI} = 30$ μm.

value as 30 μm from the probe surface. For the five bovine insulin cluster ion mass spectra, the average converged v_{ENT} is 910 ± 80 m s^{-1} and the average converged d_{GPI} is 27 ± 5 μm. Note that the value of v_{ENT} of 910 m s^{-1} is well within the range of previously reported measurements of the entrainment velocity of MALDI ions. The high linear correlation in the ΔE vs $\frac{1}{2}(m)$ plots (average $R^2 = 0.91$) combined with the reasonable agreement between the calculated entrainment velocity and previously reported values lends support to the model proposed to explain the broad component *f.t.* behavior.

The cumulative model of MALDI ion formation suggested by these results combines two distinct populations of ions formed with different dynamics. One population of ions is promptly formed and exhibits little or no mass-dependent total energy. The second population of ions exhibits both a delay in ion formation and a mass-dependent total energy resulting from an initial constant entrainment velocity. Of course, the existence of these two populations of ions requires that the translational energy of the promptly formed ions not be influenced by the constant-velocity plume of material in which delayed ionization occurs. This effect could certainly result if the prompt ions are formed at the surface of the sample and accelerated away from a denser, evolving plume of material by the strong source region electric field. (We note that promptly formed ions are observed exclusively when 'ultra-thin film' sample preparation methods are used, lending support to the contention that the prompt ions are surface formed ions.)[8]

Although elements of this two-component model of MALDI ion formation are consistent with previously suggested models (specifically, constant-velocity entrainment and delayed gas-phase ionization), several elements appear contradictory to previously suggested models. For example, previous reports have suggested that all high-mass MALDI ions produced in strong electric fields exhibit increasing deficits in total energy.[6] The existence of populations of ions which make up the sharp Gaussian component of the ion signal profiles and which have apparent mass-independent total energies approximately equal to the full acceleration potential appears to contradict this result. Furthermore, the existence of two overlapped populations of ions with different formation dynamics remains generally unexplored (although several researchers have suggested the existence of a two-component MALDI ion formation mechanism[9]).

Additional experimental support of two-component model

The implication of the suggested model that high-mass ions may have total translational energies greater than the acceleration potential was of immediate concern since this result appears to contradict previous reports. To test for high-mass ions having total translational energies greater than the acceleration potential, the source region of the TOF mass spectrometer was modified to incorporate a deceleration region immediately adjacent to the ion source [see Fig. 4(a)]. All electrodes used in these experiments had 90% transmission Ni

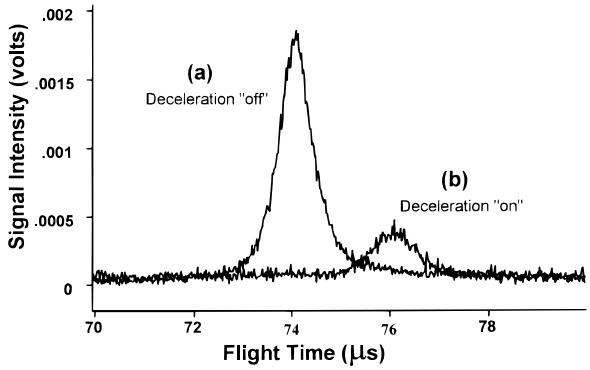

Figure 4. Single-stage acceleration of lysozyme with (a) no flight path deceleration/re-acceleration and (b) prompt deceleration/re-acceleration. The ion signal which is observed in spectrum (b) must result from ions having total energies greater than the acceleration energy of 20 000 V. These high-energy ions represent 17% of the original lysozyme signal. Note, however, that these ions are not observed when deceleration/re-acceleration is performed 40 cm down the field-free drift tube of the TOF mass spectrometer.

grids affixed to the central holes to cleanly delineate the electric fields and potentials.) The potential applied to the deceleration grid could either be set to ground (normal MALDI/TOF experiment) or, using the same power supply, to the potential applied to the ion repeller. The results of this experiment applied to the singly charged parent ion of lysozyme (m/z 14 306) produced by MALDI is shown in Fig. 4(b). Even with a voltage equivalent to the acceleration potential applied to the deceleration grid, a substantial fraction of the ions (17%) have energies greater than the acceleration potential. Note that this signal cannot be the result of metastable decay of the lysozyme parent ion. Neutral products of metastable decay would not experience deceleration and re-acceleration and would arrive at the same *f.t.* as the parent ion. Ionic products of metastable decay would necessary have total energies less than that of the parent ion and would not exceed the deceleration potential.

The apparent contradiction of this result with previous reports of high molecular mass MALDI ion energy deficits was reconciled when a similar experiment was performed with the deceleration region placed 40 cm away from the ion source region. In this experiment, no ion signal was detected upon application of the deceleration potential. Thus, it appears that the ions with total translational energies greater than the acceleration potential preferentially undergo metastable decay in the field-free drift region. Inefficient collection of the high-energy ions is inconsistent with the experimental results since these high-energy ions are collected in the prompt deceleration and re-acceleration experiment. An intriguing implication of this result is that the two populations of ions appear to have significantly different internal energies.

The existence of two populations of ions with different formation dynamics suggested by the model described in this paper was also tested in a series of two-stage acceleration MALDI experiments. An examination of Eqn (3) suggests that the total translational energy of the broad component ions should be dependent on the source region electric field, F. As the source region electric field is reduced the energy deficit resulting from delayed gas-phase ionization should decrease. Thus, if the v_{ENT} and the sharp component ion total translational energies remain constant despite changes in the source region electric field, the *f.t.* of the broad component ion relative to the sharp component ions should decrease.

Figure 5 shows the ion signal profiles of the bovine insulin BI^+ taken with a constant total acceleration of 20 000 V and a variable source region electric field. The resulting ion signal profiles with source region electric fields of (a) 20 000, (b) 10 000 and (c) 5000 V cm^{-1} are shown along with the two-component Gaussian fits to the ion signal profiles. There is a clear progressive shift in the *f.t.* of the peak maximum of the broad component ion signal from longer to shorter flight times as the source region electric field is reduced. The observed behavior is in exact agreement with that predicted from the model described in this paper.

A further insight into the mechanism of MALDI ion formation was gained in this study. Examination of the areas of the broad and sharp components of the ion signal profiles shows that the area of the sharp component relative to the broad component appears to decrease as the source region electric field is reduced. This observation suggests that the mechanism which leads to the formation of the ions which make up the sharp component of the ion signal profile may be dependent on the field strength in which the MALDI ions are formed. This is an important observation since it allows the suggested model to be reconciled with the

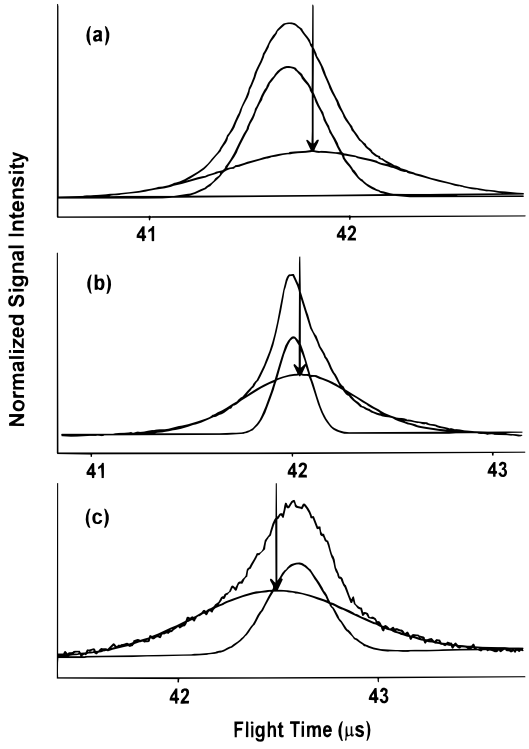

Figure 5. Ion signal profiles and the two-component Gaussian fits for the bovine insulin parent ion obtained under one- and two-stage acceleration conditions. The total acceleration is held constant at 20 000 V while the source region field strength is varied from (a) 20 000 to (b) 10 000 and (c) 5000 V cm^{-1}. Note the progressive shift of the broad component maximum (marked with an arrow) from flight times later than the sharp component to flight times shorter than the sharp component.

experimentally observed MALDI ion signal resolution enhancement under delayed extraction conditions.[10] The spatially and temporally diffuse ions formed by the gas-phase ionization process would be expected to show enhanced resolution under the space–velocity correlation conditions used in delayed extraction MALDI whereas surface-formed ions would not. If, as the results suggests, only gas-phase ions are produced in the zero-filed source region prior to the pulsed high-field extraction, then surface-formed ions do not contribute to degradation of the delayed extraction ion signal.

Finally it should be noted that we obtained essentially identical results by performing the analyses described on MALDI/TOF spectra of lysozyme cluster ions. The extracted entrainment velocities (880 ± 150 m s^{-1}) and points of gas-phase ionization (35 ± 12 μm) from the deconvolved asymmetric ion signal profiles are in good agreement with the data presented here. Furthermore, experimental evidence which supports the two-component model of MALDI ion formation has been obtained in a separate investigation.[11] These data were obtained by measuring the kinetic energies of MALDI ions in an electrostatic analyzer TOF mass spectrometer. Extensive analysis of the kinetic energy–flight time behavior of the MALDI ions observed in these experiments leads to the development of an essentially identical two component model of MALDI ion formation.

CONCLUSIONS

The results of the flight time and ion signal profile analyses applied to bovine insulin cluster ion signals strongly suggest a two-component model of MALDI ion formation. In many ways the implications of this model of MALDI ion formation allow the reconciliation of a variety of previous seemingly contradictory studies of the dynamics of MALDI ion formation. The dynamics of one component of the MALDI ion suggests that these ions are desorbed as preformed ions or formed very near the probe surface and are acceleratrd to essentially mass-independent total translational energies. The dynamics of the second component of the MALDI ions suggest that these ions are the product of delayed gas-phase ionization in a plume of material moving at a constant velocity. The total translational energy of the ions produced by this process is dependent on the mass of the ions, the entrainment velocity, the source region electric field strength and the point in the source region at which ionization occurs. As a result, across a broad mass range, lower mass ions may have total translational energy deficits whereas higher mass ions have total translational energy excesses. The combination of ions produced by these two mechanisms, along with the ancillary experiments and observations described, provide a comprehensive picture of MALDI ion formation which easily accounts for the observed cluster ion signal profiles and also the results of a wide variety of other experimental studies of MALDI ion formation dynamics.

Acknowledgements

This work was supported by grants from the United States Department of Energy, Division of Chemical Sciences, Office of Basic Energy Science and the National Science Foundation.

REFERENCES

1. R. W. Nelson, D. Dogruel and P. Williams *Rapid Commun. Mass Spectrom.* **8**, 627 (1994).
2. G. R. Kinsel, L. M. Preston and D. H. Russell, *Biol. Mass Spectrom.* **23**, 205 (1994).
3. D. W. Marquardt, *J. Soc. Ind. Appl. Math.* **11**, 431 (1963).
4. R. C. Beavis and B. T. Chait, *Chem. Phys. Lett.* **181**, 479 (1991).
5. (*a*) Y. Pan and R. J. Cotter, *Org. Mass Spectrom.* **27**, 3 (1992); (b) T. Huth-Fehre and C. Becker, *Rapid Commun. Mass Spectrom.* **5**, 378 (1992); (c) D. Kirsch, B. Spengler and R. D. Kaufmann, in *Proceedings of the 41st ASMS Conference on Mass Spectrometry and Allied Topics*, San Francisco, CA, 1993, p. 670a; (d) A. Verentchikov, W. Ens, J. Martens and K. G. Standing, in *Proceedings of the 40th ASMS Conference on Mass Spectrometry and Allied Topics*, Washington, DC, 1992, p. 360.
6. J. Zhou, W. Ens, K. G. Standing and A. Verentchikov, *Rapid Commun. Mass Spectrom.* **6**, 671 (1992).
7. A. E. Giannakopulos, D. J. Reynolds, T.-W. Dominic Chan, A. W. Colburn and P. J. Derrick, *Int. J. Mass Spectrom. Ion Processes*, **131**, 67 (1994).
8. R. D. Edmondson, K. K. Campo and D. H. Russell in *Proceedings of the 43rd ASMS Conference on Mass Spectrometry and Allied Topics*, Atlanta, GA, 1995, p. 1246.
9. (a) A. P. Quist, T. Huth-Fehre and B. U. R. Sundqvist, *Rapid Commun. Mass Spectrom.* **8**, 149 (1994); (b) A. Westman, P. Demirev, T. Huth-Fehre, J. Bielawski and B. U. R. Sundqvist, *Int. J. Mass Spectrom. Ion Processes* **130**, 107 (1994); (c) V. Bökelmann, B. Spengler and R. Kaufmann, *Eur. Mass Spectrom.* **1**, 81 (1995); (d) K. Riahi, G. Bolbach, A. Brunot, F. Breton, M. Spiro and J.-C. Blais, *Rapid Commun. Mass Spectrom.* **8**, 242 (1994).
10. (a) S. M. Colby, T. B. King and J. P. Reilly, *Rapid Commun. Mass Spectrom.* **8** 865 (1994); (b) T. B. King, S. M. Colby and J. P. Reilly, *Int. J. Mass Spectrom. Ion Processes*, **145**, L1 (1995); (c) M. P. Christian, S. M. Colby, L. Giver, C. T. Houston, R. J. Arnold, A. D. Ellington and J. P. Reilly, *Rapid Commun. Mass Spectrom.* **9**, 1061 (1995); (d) R. S. Brown and J. J. Lennon, *Anal. Chem.* **67**, 1998 (1995); (e) R. S. Brown and J. J. Lennon, *Anal. Chem.* **67**, 3990 (1995).
11. G. R. Kinsel and D. H. Russell, in preparation.

